Title
Ozone, hydroperoxides, oxides of nitrogen, and hydrocarbon budgets in the marine boundary layer over the South Atlantic

Journal
Journal of Geophysical Research, 101(D19)

ISSN
0148-0227

Authors
Heikes, Brian
Lee, Meehye
Jacob, Daniel
et al.

Publication Date
1996-10-30

DOI
10.1029/95jd03631

JOURNAL OF GEOPHYSICAL RESEARCH, VOL. 101, NO. D19, PAGES 24,221–24,234, OCTOBER 30, 1996

Ozone, hydroperoxides, oxides of nitrogen, and hydrocarbon budgets in the marine boundary layer over the South Atlantic

Brian Heikes,[1] Meehye Lee,[1] Daniel Jacob,[2] Robert Talbot,[3] John Bradshaw,[4] Hanwant Singh,[5] Donald Blake,[6] Bruce Anderson,[7] Henry Fuelberg,[8] and Anne M. Thompson[9]

Abstract. The NASA GTE TRACE A mission sampled air over the South Atlantic and western Indian Oceans. Thirteen flight legs were flown within the marine boundary layer (MBL). The MBL was typically the cleanest air sampled (e.g., $CH_4 < 1680$ ppb, $CO < 70$ ppb, $C_2H_6 < 400$ ppt, $C_3H_8 < 40$ ppt, $NO_x < 15$ ppt, and midday $NO < 5$ ppt) but was overlain by polluted air. The photochemistry of the MBL was influenced by oceanic emissions, surface deposition, and entrainment of pollutants from aloft. Chemical budgets were constructed for several species in the MBL in order to investigate these effects and are presented for ethane, ethylene, propane, propylene, *n*-butane, formic acid (HFo), methylhydroperoxide (CH_3OOH), oxides of nitrogen (i.e., NO, NO_2, PAN, HNO_3), hydrogen peroxide (H_2O_2), and ozone (O_3). A photochemical point model was used to evaluate local chemical production and loss. An entrainment model was used to assess material exchange between the lower free troposphere (FT) and the MBL and a resistance deposition model was used to evaluate material exchange across the air-sea interface. The results suggested the ocean to be the source of measured alkenes in the MBL and to be the most likely source of the shorter-lived alkanes: propane and *n*-butane. Ethane was the only hydrocarbon for which input from aloft may have exceeded its photochemical destruction. The estimated hydrocarbon sources from the ocean were in agreement with prior analyses. Transport from the lower FT together with surface loss could not account for measured concentrations of CH_2O, HFo, and HNO_3. The transport of peroxyacetylnitrate (PAN) from the FT to the MBL exceeded the rate of HNO_3 production and was more than sufficient to maintain observed NO_x levels without having to invoke an oceanic source for NO. The flux of NO_x, PAN, and HNO_3 was in balance with the surface deposition flux of HNO_3. However, the predicted rates of HNO_3 formation from the oxidation of NO_2 and HNO_3 entrainment from aloft were inadequate to maintain observed levels of HNO_3 unless HNO_3 was partitioned between the gas phase and a more slowly depositing aerosol phase. The estimated dry deposition flux of HNO_3 to the South Atlantic during TRACE A, $2–4 \times 10^9$ molecules cm^{-2} s^{-1}, was about 10 times the annual average estimate for this region. The destruction of O_3 within the MBL was found to be exceeded by transport into the MBL from aloft, $6 \pm 2 \times 10^{10}$ compared to $11 \pm 10 \times 10^{10}$ molecules cm^{-2} s^{-1}. The principal O_3 destruction process was mediated by the formation and surface deposition of H_2O_2 and CH_3OOH, $4 \pm 4 \times 10^{10}$ and $1.1 \pm 0.5 \times 10^{10}$ molecules cm^{-2} s^{-1}. The direct loss of O_3 to the sea surface was estimated to be $1.7 \pm 0.2 \times 10^{10}$ molecules cm^{-2} s^{-1}. CH_3OOH was lost to the sea and transported into the FT from the MBL. Its first-order loss rate was estimated to be 7×10^{-6} s^{-1} for a mean MBL height of 700 m. H_2O_2 and CH_2O losses from the MBL were estimated at rates of 1.3×10^{-5} s^{-1} for both species. The inclusion of surface deposition improved the agreement between predicted and measured concentrations of HNO_3, CH_3OOH, H_2O_2, and CH_2O. However, model CH_2O remained significantly greater than that measured in the MBL.

[1]Center for Atmospheric Chemistry Studies, Graduate School of Oceanography, University of Rhode Island, Narragansett.
[2]Harvard University, Cambridge, Massachusetts.
[3]University of New Hampshire, Durham.
[4]Georgia Institute of Technology, Atlanta.
[5]NASA Ames Research Center, Moffet Field, California.
[6]University of California, Irvine.
[7]NASA Langley Research Center, Hampton, Virginia.
[8]Florida State University, Tallahassee.
[9]NASA Goddard Space Flight Center, Greenbelt, Maryland.

Paper number 95JD03631.
0148-0227/96/95JD-03631$09.00

1. Introduction

The NASA GTE Transport and Atmospheric Chemistry near the Equator—Atlantic Experiment (TRACE A) was an investigation in to the causes of high tropospheric ozone (O_3) concentrations observed over the South Atlantic in the months of September and October [*Fishman et al.*, 1990, this issue(a)]. The TRACE A study area included the continents of South America and Africa and the South Atlantic and western Indian Oceans. The experiment occurred in September and October 1992. The NASA DC-8 aircraft was used as a platform to measure O_3 and the distribution of key-related species throughout the entire depth of the troposphere. On 7 of the 19 flights a total of 13 legs were flown in the marine boundary layer (MBL). We present in this paper MBL chemical budgets for O_3, light hydrocarbons, oxides of nitrogen, and a few photochemical products over the South Atlantic and western Indian Oceans. TRACE A results related to high O_3 throughout the tropospheric column are presented in companion articles [e.g., *Fishman et al.*, this issue(b); *Thompson et al.*, this issue; *Jacob et al.*, this issue; *Krishnamurti et al.*, this issue].

The remote MBL is recognized for its role in the destruction of tropospheric O_3, the antithesis of the primary TRACE A mission. *Lenschow et al.* [1982], *Kawa and Pearson* [1989], and *Paluch et al.* [1994] evaluated the vertical flux of O_3 at the top of the MBL and within the MBL. They showed the MBL over the Gulf of Mexico and the eastern North Pacific to be a sink for tropospheric O_3. Ozone loss was postulated to be the result of photochemical destruction and ozone destruction/absorption at the ocean's surface. *Noone et al.* [1995] examined O_3 in and above the MBL over the North Atlantic in two Lagrangian experiments near the Azores. They could not resolve net O_3 production from surface deposition and entrainment. Modeling studies by *Liu et al.* [1983] and *Thompson et al.* [1993] have shown the net destruction of ozone in the MBL to be photochemically mediated with O_3 replacement from the overlying free troposphere (FT). These chemical models were applied to observations from the equatorial Pacific Ocean, where nitric oxide (NO) concentrations were less than a few ppt. *Ayers et al.* [1992] and *Ayers et al.* [1995] examined the correlation of O_3 and H_2O_2 over diel and annual cycles at Cape Grimm, Tasmania, and showed the daytime destruction of O_3 to be accompanied by a stoichiometric increase in peroxides (most likely hydrogen peroxide and a major fraction of methylhydroperoxide). They further suggested that replacement O_3 was mixed into the MBL from aloft, while the peroxides were lost to the ocean's surface. The TRACE A measurements and photochemical model results permitted an evaluation of the rate and mechanism of net O_3 production in the MBL over the South Atlantic under similar low NO conditions.

Several investigations have attempted to evaluate the oceanic flux of hydrocarbons into the atmosphere and their impact on atmospheric chemistry, particularly O_3 and hydroxyl (HO). A combination of atmospheric measurements, seawater measurements, air-sea exchange rates, and photochemical models have been used to infer hydrocarbon fluxes over the equatorial Pacific [*Donahue and Prinn*, 1993; *Thompson et al.*, 1993], the North and South Pacific [*Lamontagne et al.*, 1974], the Atlantic [*Rudolph and Johnen*, 1990; *Plass et al.*, 1992], the Indian Ocean [*Bonsang et al.*, 1988], and in the remote marine atmosphere [*Donahue and Prinn*, 1990]. *Bonsang et al.* [1991] made hydrocarbon measurements up to an altitude of 1600 m from which they investigated both oceanic emissions and MBL-FT exchange at an island site in the South Pacific. Nevertheless, measurements and oceanic flux estimates remain sparse in time and location over the ocean. Although few in number, the evaluated oceanic hydrocarbon emissions span orders of magnitude. A combination of model results and measurements are applied below in an investigation of the relative contribution of FT-MBL exchange and oceanic emissions in establishing hydrocarbon concentrations in the MBL over the South Atlantic.

Oxides of nitrogen along with hydrocarbons are central to defining oxidant species and their concentrations in the atmosphere. The remote MBL is one of the few regions of the world wherein noontime NO levels below 5 ppt are consistently found [*McFarland et al.*, 1979; *Torres and Thompson*, 1993]. *Zafiriou and McFarland* [1981] and *Torres and Thompson* [1993] proposed a weak photolytic source of atmospheric NO from nitrate rich ocean waters. TRACE A NO concentrations in the MBL were also below 5 ppt under daylight conditions [*Smyth et al.*, this issue]. NO, nitrogen dioxide (NO_2), peroxyacetylnitrate (PAN), and nitric acid (HNO_3) were typically observed to increase in going from the MBL to the FT [*Singh et al.*, this issue], which suggested that the downward flux of nitrogen oxides could be an important source of MBL nitrogen oxides in the TRACE A study location.

While the deposition of HNO_3 to the ocean removes reactive nitrogen from the troposphere, thereby limiting net oxidant production, the downward flux of HNO_3 and the conversion of NO_2 to HNO_3 in the MBL has important biological implications. Biological productivity in the oligotrophic ocean is considered to be limited by the availability of fixed nitrogen and the atmosphere may be a source of this macronutrient [*Duce et al.*, 1991]. The TRACE A oxides of nitrogen data allowed estimates of the flux of HNO_3 to the South Atlantic to be made and allowed a reexamination of earlier estimates of the air-sea input of fixed nitrogen over this region.

Hydrogen peroxide, CH_3OOH, and CH_2O measurements have been used to validate photochemical model odd hydrogen (e.g., HO, HO_2, RO_2) chemistry through the comparison of observed and predicted concentrations. The comparisons with airborne data above the boundary layer are in agreement within stated measurement and kinetic uncertainties [*Jacob et al.*, this issue; *Crawford et al.*, 1995]. However near the Earth's surface, models and measurements diverge with the models typically indicating higher values than observed [*Lowe and Schmidt*, 1983; *Thompson et al.*, 1993; *Crawford et al.*, 1995; *Jacob et al.*, this issue], and surface deposition of the more highly soluble species, e.g., CH_2O, HNO_3, and H_2O_2, has often been invoked to explain these differences. The suite of the more soluble species measured in TRACE A (H_2O_2, CH_3OOH, CH_2O, HNO_3, and HFo) together with the measurements of O_3, NO, and hydrocarbons permitted us to examine this assumption and test for consistency between the deposition of species with short photochemical timescales (e.g., H_2O_2, CH_3OOH, or CH_2O) and those with longer photochemical timescales (e.g., O_3, HNO_3 or HFo). These data and their analysis provide additional constraints on the models and, if successful, place greater confidence in other model products (e.g., HO or net O_3 production).

2. Methodology

The location of the TRACE A MBL flight legs is shown in Figure 1. Specific MBL cases are identified by lowercase letters. Capital letters indicate aircraft bases of operation: A,

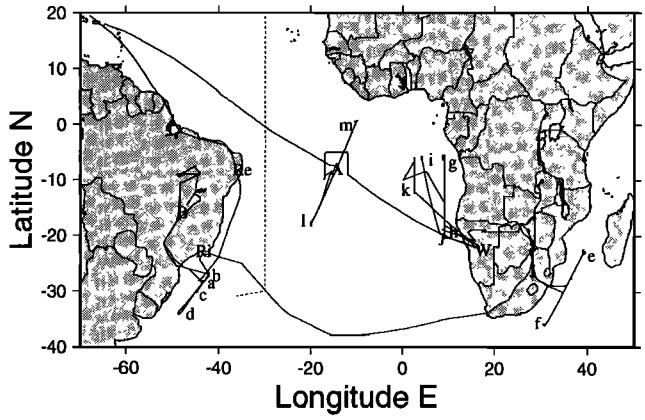

Figure 1. Map of the TRACE A study region showing the location of marine boundary layer legs (lowercase letters), DC-8 flight tracks (solid line), the track of the 1988 *Polarstern* Cruise ANT VII/1 (dashed line), bases of operation (Re, Recife; Ri, Rio de Janeiro; J, Johannesburg; W, Windhoek; and A, Ascension Island).

Ascension Island; J, Johannesburg; Re, Recife; Ri, Rio de Jenero; W, Windhoek. The lower atmosphere during TRACE A was characterized by a strong thermal inversion at the top of the MBL at which the specific humidity (q) of the air decreased markedly. Often, the MBL was capped by stratus clouds which are a prominent feature of the South Atlantic MBL. The height of the MBL (Z_{MBL}) was defined by the temperature inversion and decrease in q and encompassed the marine stratus and cumulus clouds. A combination of dropsonde data (see discussion by *Fuelberg et al.* [this issue(a)]), differential absorption lidar (DIAL) data [*Browell et al.*, this issue], and aircraft observations were used to establish Z_{MBL}. Air parcel trajectories for the MBL, calculated using the procedures of *Fuelberg et al.* [this issue(b)], indicated sampled air masses to have been over the ocean for at least the prior 4 days. Further, the concentrations of NO, CO, CH_4, and other chemical data suggested it to be relatively unimpacted by recent continental emissions. Chemical data and air trajectories for the overlying FT indicated this air to have come from over the continents within the past 1 to 2 days [*Pickering et al.*, this issue] and the chemical data suggested that it contained partially processed continental biomass and industrial emissions [*Talbot et al.*, this issue; *Mauzerall et al.*, 1996; *Blake et al.*, this issue]. Table 1 lists the MBL cases, locations, times, MBL height (Z_{MBL}), and other chemical data.

The complete suite of chemical and meteorological measurements made onboard the DC-8 during TRACE A is listed by *Fishman et al.* [this issue(a)]. Specific chemical measurements used in this study are presented briefly below. Nitric oxide and NO_2 were measured using two-photon laser-induced fluorescence [*Smyth et al.*, this issue]. Hydrocarbon samples (specifically ethane, ethene, propane, propene, and n-butane or C_2H_6, C_2H_4, C_3H_8, C_3H_6, and n-C_4H_{10}, respectively) were collected in stainless-steel canisters and analyzed using the techniques and procedures outlined by *Blake et al.* [this issue]. O_3 was measured using a NO-O_3 chemiluminescence method [*Collins et al.*, this issue]. H_2O_2 and CH_3OOH were collected in aqueous solution and analyzed using a high-pressure liquid chromatography system [*Lee et al.*, 1995]. CH_2O was collected in aqueous solution using a coil collector and was analyzed by the method of *Lazrus et al.* [1988]. HNO_3 and formic acid (HFo) were collected in aqueous solution using mist chambers and analyzed by ion chromatography [*Talbot et al.*, this issue].

A slab model [after *Lenschow et al.*, 1982] was used to analyze MBL chemical budgets. In this model, the time rate of change of a chemical constituent in the MBL slab ($dC_{i,MBL}/dt$, molecules cm^{-3} s^{-1}) is described by its local photochemical production and loss ($P_{i,MBL}$ and $L_{i,MBL}$, molecules cm^{-3} s^{-1}), its flux across the air-sea interface ($F_{i,AS}$, molecules cm^{-2} s^{-1}), and its flux across a surface defining the top of the MBL ($F_{i,MBL}$, molecules cm^{-2} s^{-1}):

$$dC_{i,MBL}/dt = P_{i,MBL} - L_{i,MBL} - F_{i,MBL}/Z_{MBL} - F_{i,AS}/Z_{MBL}$$

where i denotes a specific chemical species. Horizontal advection was assumed to be negligible on the timescale of a day or 3, which was of the order of the chemical relaxation times of the species listed above. Figure 2 shows a schematic of the lower atmosphere and the transport processes which we have included.

The flux at the top of the MBL is represented by an entrainment velocity (K_e) times the difference in concentration between the FT and MBL:

$$F_{MBL} = K_e^*(C_{i,FT} - C_{i,MBL})$$

where C_i has units of molecules cm^{-3}. K_e was assumed to be equal to 0.5 cm s^{-1} and was estimated from the work of *Lenschow et al.* [1982], *Kawa and Pearson* [1989], *Paluch et al.* [1994], and *Bretherton and Siems* [1994], describing the flux of O_3 across the top of the MBL under meteorological conditions

Table 1. Marine Boundary Layer Cases

Case	Flight	Julian Day	Start Time, sec-UT	Stop Time, sec-UT	Latitude, North	Longitude, East	Pressure, hPa	Wind Speed ~300 m, m s^{-1}	Wind Speed 10 m, m s^{-1}	MBL Height, m
a	5	268	56010	59910	−28.90	−44.10	973	18	13	450
b	8	275	52350	54570	−27.10	−42.00	978	8	6	500
c	8	275	55950	57930	−30.03	−44.90	970	12	9	500
d	8	275	60390	62610	−33.98	−48.30	977	12	9	500
e	11	283	32970	35490	−23.40	38.85	983	8	6	600
f	11	383	42810	45270	−35.55	31.30	993	8	6	600
g	13	288	36750	39630	−6.60	8.75	978	5	4	900
h	13	288	43950	47730	−19.20	9.00	979	8	6	700
i	14	289	38190	41070	−6.20	4.05	979	4	3	1100
j	14	289	46350	50130	−19.88	8.58	982	12	9	1000
k	15	292	51330	54510	−11.67	2.50	976	5	4	1000
l	17	296	38610	41430	−17.30	−19.70	984	7	6	500
m	17	296	51270	54090	0.00	−10.40	975	9	7	700

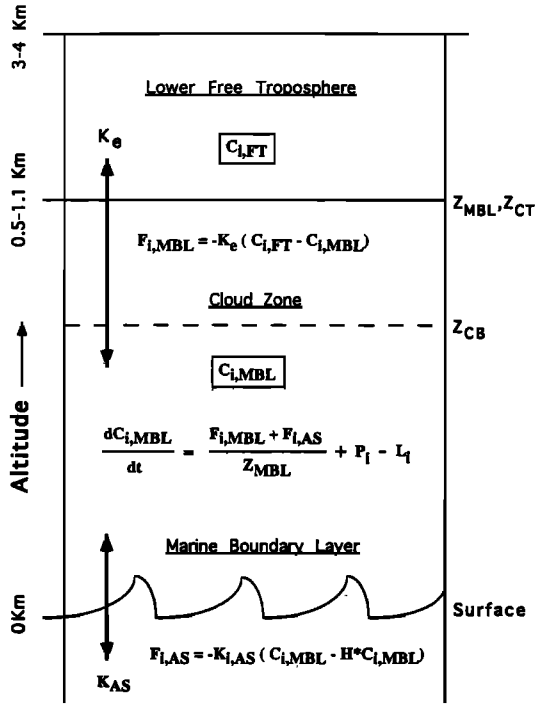

Figure 2. Schematic of the three-layer lower-atmosphere transport model used in the marine boundary layer (MBL) chemical budget studies [after *Lenschow et al.*, 1983].

quite similar in vertical stability to those encountered during TRACE A. The value assigned to K_e was also consistent with studies examining the development of marine stratus clouds and O_3 [*Penc and Albrecht*, 1987; *Wang and Albrecht*, 1994; *Bretherton et al.*, 1995]. K_e was taken to be independent of chemical species. The lower FT composition, $C_{i,FT}$, was taken from the measurements and reflected the variance in air mass source regions, discussed above with respect to the MBL and lower FT and present at other altitudes in a given column [*Pickering et al.*, this issue; *Fuelberg et al.*, this issue(b)].

The flux of HNO_3, HFo, CH_3OOH, H_2O_2, and CH_2O into the ocean was estimated using a deposition velocity ($K_{i,AS}$) times the MBL concentration:

$$F_{i,AS} = K^*_{i,AS}(C_{i,MBL} - C^*_{i,AS})$$

The oceanic equivalent gas phase concentration in the upper ocean, $C^*_{i,AS}$, was assumed to be negligible for the species listed. $K_{i,AS}$ was evaluated using the simplified thin-film parameterized model of *Duce et al.* [1991]. Air-sea transfer was assumed to be limited by atmospheric turbulence for all but CH_3OOH, which has a significantly lower solubility in water [*O'Sullivan et al.*, 1995], than the other species. Hence its uptake depends upon both an atmospheric transport velocity, k_a, and an oceanic transport velocity, k_w. This scheme required the wind speed and concentrations at 10-m elevation. The 10-m wind speed has been calculated from aircraft-measured wind speed (nominally 300-m elevation), assuming a logarithmic wind profile and the parameterization given by *Wu* [1995]. These wind speeds are listed in Table 1 and were nearly identical to climatological values [*U.S. Navy*, 1978, 1976]. A typical wind speed was 7 m s^{-1}. At 7 m s^{-1} the resulting deposition velocity for CH_3OOH is 0.5 cm s^{-1} and is 0.88 cm s^{-1} for the other gases. *Thompson and Lenschow* [1984] showed through a modeling investigation that the concentration of a soluble gas (e.g., HNO_3) at 10-m height is within a few percent of its concentration at 100 m or higher and the concentrations at 300 m have been used without modification to calculate surface fluxes. The assumptions related to surface fluxes could be compromised if flow separation has developed (C. S. Bretherton, personal communication) and the estimated fluxes would then reflect upper limit values. Flow separation is associated with relative deep and mature MBLs, which are characterized by marine cumulus clouds. The bulk of the MBL cases here were overlain by marine stratus, which suggested a continuous MBL flow regime connecting the surface flux layer to the MBL cloud layer. Hence the assumptions above appeared reasonable.

The diel-average photochemical point model of *Jacob et al.* [this issue] was used to evaluate local MBL chemistry (i.e., $P_{i,MBL}$ and $L_{i,MBL}$). Parameterizations of vertical fluxes, such as those just described, are not included in the model. Odd oxygen (sum of O_3, O, NO_2, HNO_4, $2*NO_3$, and $3*N_2O_5$), H_2O_2, CH_3OOH, and HNO_3 production rates were calculated along with the concentrations of HO, perhydroxyl (HO_2), H_2O_2, CH_3OOH, CH_2O, HNO_3, NO_2, and PAN. The model calculations were performed using a merged time series of the aircraft data indexed to the NO sample times [see *Jacob et al.*, this issue]. The availability of hydrocarbon measurements limited the number of points which could be explicitly simulated, and in order to enhance the number of model-measurement points, the model was run assuming fixed background hydrocarbon concentrations [*Jacob et al.*, this issue].

The MBL chemical concentrations were taken from the NO-merged product for consistency with the photochemical point model [*Jacob et al.*, this issue] or, if available, directly from actual observations entirely within the MBL. However, estimating lower FT concentrations was more difficult. Individual species measurements were made with different instrument duty cycles and at variable intervals. This, together with the aircraft ascent/descent rate nominally 7 m s^{-1}, made it necessary to infer $C_{i,FT}$ from observations between Z_{MBL} and 4000 m. This treatment was analogous to those used by *Paluch et al.* [1994] and *Wang and Albrecht* [1994], wherein they used mean concentrations between Z_{MBL} and a reference height to calculate material fluxes at the MBL. Table 2 lists the MBL and FT hydrocarbon concentrations for the 13 cases identified. Table 3 lists MBL and FT concentrations for H_2O_2, O_3, CO, CH_3OOH, CH_2O, HFo, HNO_3, PAN, and NO_x (sum of NO and NO_2). Figures 3 and 4 show vertical profiles for these species for cases *d* and *i* from flights 8 and 14 off the coasts of Brazil and Gabon. Species variation within the MBL and during descent and ascent at each end of a MBL leg are illustrated by these figures. The dashed line shows the height of the MBL.

The species examined were chosen because of their relevance to photochemistry in the MBL and to check for consistency among measurements, photochemical model results, and transport models. They represent a mix of species with different aqueous solubilities, sources, and photochemical lifetimes.

3. Results

3.1. O_3 – H_2O_2 – CH_3OOH

According to current understanding, destruction of ozone in the MBL is thought to proceed through the following se-

Table 2. Light Hydrocarbon Concentrations, ppt

	Marine Boundary Layer						4 km to Top of MBL					
Case	C_2H_6	C_2H_4	C_3H_8	C_3H_6	n-C_4H_{10}	i-C_4H_{10}	C_2H_6	C_2H_4	C_3H_8	C_3H_6	n-C_4H_{10}	i-C_4H_{10}
a	450	20	200	4	70	40	650	140	400	6	150	90
b	330	5	25	2	5	2	320	1	10	<1	<1	<1
c	na	na	na	na	na	na	330	3	14	<1	1	<1
d	340	6	30	4	6	5	320	2	10	2	<1	<1
e	325	11	12	4	<1	<1	500	8	25	2	3	<1
f	370	8	40	5	9	6	390	7	30	2	5	4
g	325	15	12	5	2	<1	850	18	50	4	4	2
h	315	15	17	5	2	<1	410	5	18	6	<1	<1
i	310	11	10	4	<1	<1	700	10	40	5	3	<1
j	290	11	14	4	2	1	600	16	30	8	1	<1
k	310	12	14	4	<1	<1	550	7	25	3	1	<1
l	310	18	15	6	1	<1	500	7	20	5	1	<1
m	320	21	13	5	<1	<1	475	15	20	4	2	1

quence: (1) transport of O_3 from the FT to the MBL, (2) ozone photolysis to O^1D,

$$O_3 + h\nu \rightarrow O_2 + O^1D$$

(3) O^1D reaction with water vapor to produce HO,

$$O^1D + H_2O \rightarrow 2HO$$

(4) HO reacts with CO, CH_4, or CH_2O to yield HO_2 or CH_3OO,

$$HO + CO \rightarrow + O_2 \rightarrow HO_2 + CO_2$$

$$HO + CH_4 \rightarrow + O_2 \rightarrow H_2O + CH_3OO$$

Table 3a. Marine Boundary Layer Concentration, ppt

Case	CO, ppb	O_3, ppb	NO_x,[a]	HNO_3	PAN	H_2O_2	CH_3OOH	HFo	CH_2O
a	63	23	14	90	11	420	960	930	230
b	61	27	6	90	2	4920	1000	220	na
c	na	28	na	30	na	4800	1300	100	na
d	61	26	6	70	3	4350	1055	350	na
e	70	29	7	190	2	940	1035	340	140
f	61	30	9	150	7	690	620	540	na
g	76	25	8	280	3	1700	1380	770	na
h	66	32	11	230	3	960	770	430	<43
i	65	29	9	190	2	1580	1280	470	<44
j	61	22	11	150	1	1790	920	360	<44
k	64	25	12	280	2	1180	1140	900	77
l	65	26	<5	180	2	1010	1240	420	<47
m	88	27	<5	190	2	270	1580	420	<47
Average	67	27	8[b]	160	3	1900	1100	480	
s.d.	8	3	4[b]	70	3	1600	250	240	

[a]NO_x is the diel-average model value based upon measured NO.
[b]A value of 3 was substituted for <5 in calculating the average and standard deviation.

Table 3b. Four Kilometers to Marine Boundary Layer Concentrations, ppt

Case	CO, ppb	O_3, ppb	NO_x,[a]	HNO_3	PAN	H_2O_2	CH_3OOH	HFo	CH_2O
a	140	55	160	550	1100	4000	1300	2200	650
b	66	40	25	100	20	6000	1000	560	na
c	71	38	25	40	55	4800	1100	500	na
d	65	37	20	60	15	1500	500	250	na
e	90	55	50	250	160	1500	500	1650	150
f	73	45	25	110	60	300	400	650	na
g	180	65	75	400	400	6000	1900	4000	200
h	95	55	65	400	100	1700	750	1750	na
i	155	58	65	350	350	4500	1700	1700	na
j	125	60	65	400	350	2500	1000	2000	na
k	115	70	65	450	120	3400	1400	2700	na
l	85	70	35	250	40	1100	650	650	na
m	100	50	70	350	80	3900	1300	900	130
Average	100	55	60	280	220	3200	1000	1500	
s.d.	35	10	35	160	300	1800	450	1000	

[a]NO_x is the diel-average model value based upon measured NO.

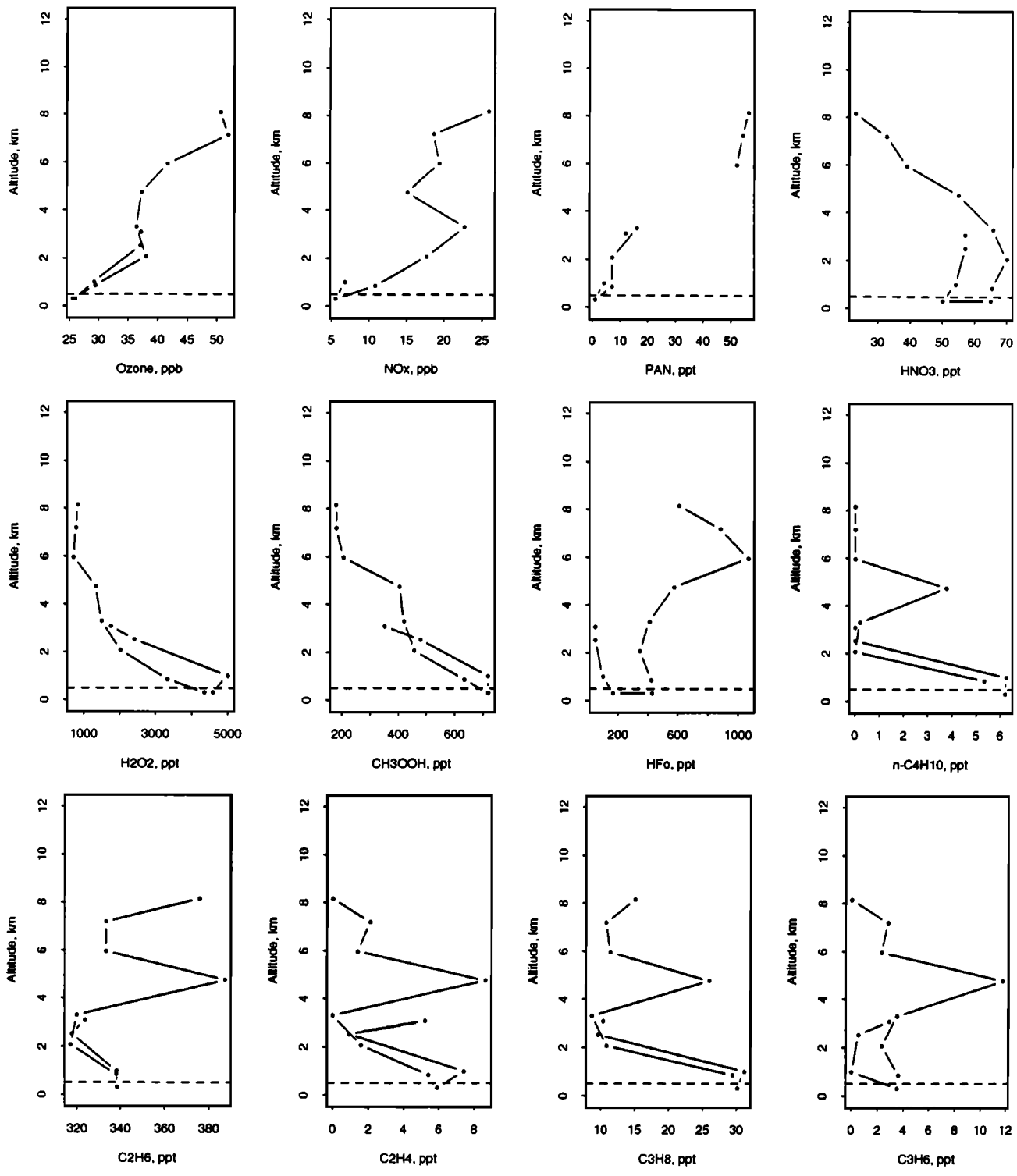

Figure 3. Vertical profiles of O_3, NO_x, PAN, HNO_3, H_2O_2, CH_3OOH, HFo, C_2H_6, C_2H_4, C_3H_8, C_3H_6, and n-C_4H_{10} for MBL case *d* off the coast of southern Brazil. The dashed horizontal line indicates MBL height. Descent, ascent, and MBL leg data are shown with lines connecting consecutive points in time. Table 1 lists MBL cases.

(5) dismutation of HO_2 and CH_3OO to make H_2O_2 and CH_3OOH,

$$2HO_2 \rightarrow H_2O_2 + O_2$$

$$HO_2 + CH_3OO \rightarrow CH_3OOH + O_2$$

and (6) subsequent removal of H_2O_2 or CH_3OOH via surface deposition or reaction with HO. This is schematically shown in Figure 5. The rates shown indicate averages and standard deviations for 12 of the 13 cases (case *c* was not included because of the aircraft's short duration in the MBL and the consequent absence

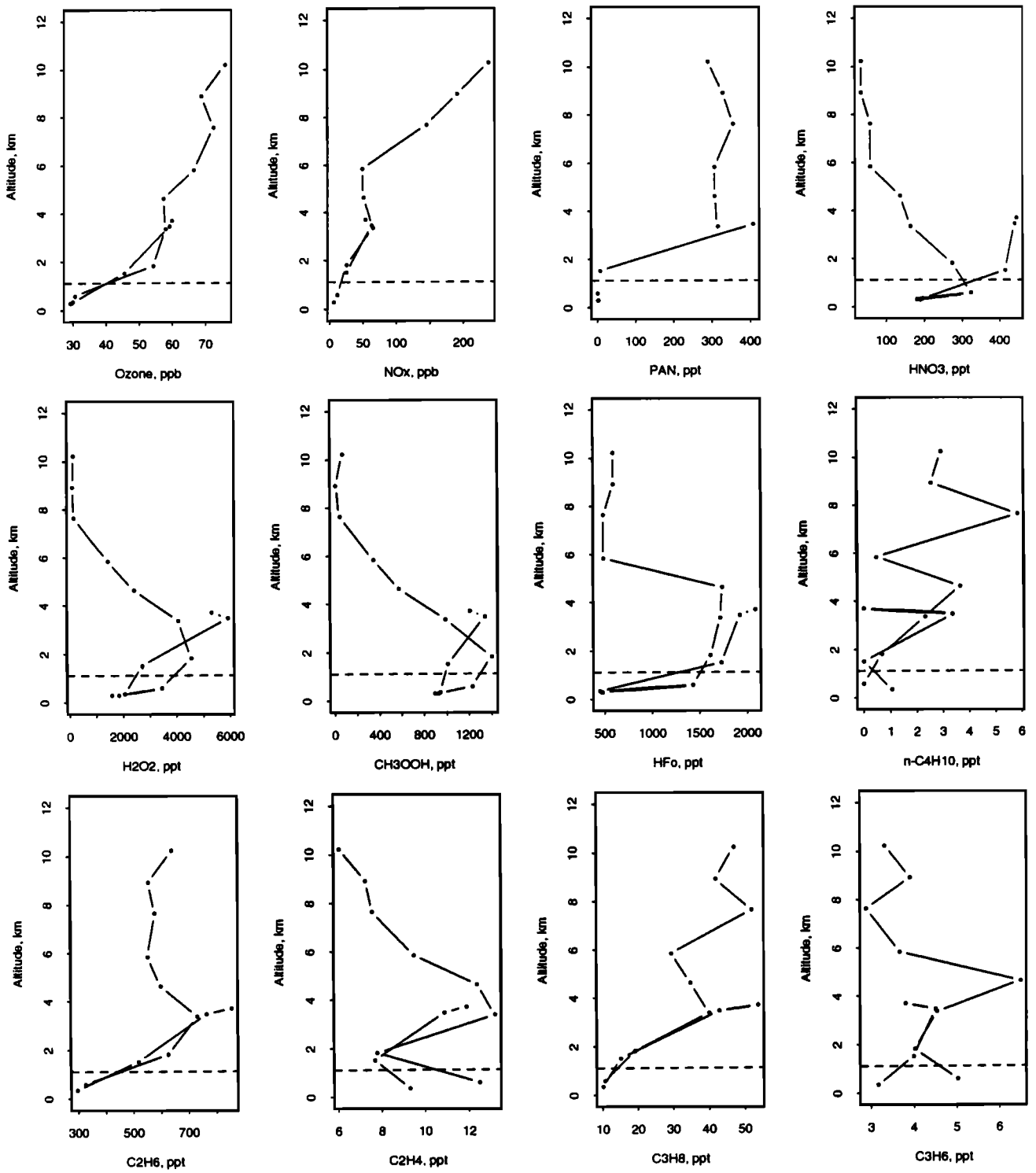

Figure 4. Same as Figure 3 except for MBL case *i* off the coast of Gabon.

of key species measurements). The loss of O_3 in the remote atmosphere proceeded primarily through hydroperoxide formation, with a smaller contribution ascribable to surface deposition ($K_{O_3,AS}$ = 0.026 [*Kawa and Pearson*, 1989]). Note that the loss of O_3 in the MBL was more than compensated for by the transport of O_3 into the MBL from aloft. This MBL-column excess was on average ~450 × 10^8 molecules cm^{-2} s^{-1}, which for a mean column height of 700 m corresponded to an O_3 increase of 1.5 ppb d^{-1}. The MBL-column O_3 loss rate was ~650 × 10^8 molecules cm^{-2} s^{-1}, which corresponded to 2.2 ppb d^{-1} and gave a mean O_3 MBL lifetime of 12 days.

The hydroperoxide budget is also shown in Figure 5. Figure 6 demonstrates the 1:1 relationship between ozone destruction and hydroperoxide production predicted by the model for all of the cases (more than 13 points are shown due to the fact that some legs had more than one calculable model point). This result for the MBL represented a unique combination of very low nitrogen oxide concentrations and moderate to high water

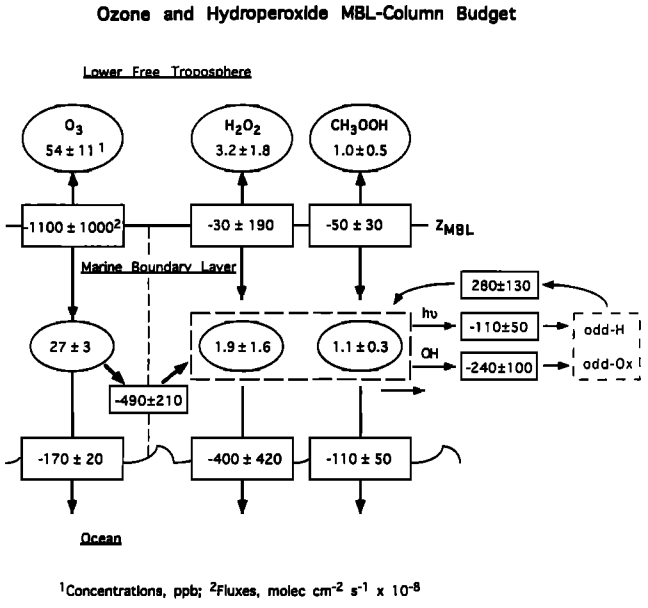

Figure 5. MBL budget of O_3, H_2O_2, and CH_3OOH. Values in rectangles give the average ± s.d. (standard deviation) of the vertical fluxes for the 13 MBL cases (molecule cm^{-2} s^{-1} × 10^{-8}). Negative flux values indicate net downward movement of material and vice versa. The transfer of odd oxygen from O_3 to the hydroperoxides is shown for the MBL by the dashed rectangle and vertical line. Values in ellipses give the average ± s.d. of the species concentration (ppb) for the free troposphere (FT) and MBL.

vapor concentrations. The total NO_x concentration was less than 15 ppt and the specific humidity (q), was >5 g kg^{-1} for all cases. The minimum hydroperoxide production rate in humid air, $q > 5$, regardless of NO_x concentration, was 1.4 ppb d^{-1} and corresponded to a net MBL column production of 280 × 10^8 molecules cm^{-2} s^{-1}. This represents a baseline production rate to which the contribution from net O_3 destruction should be added. The photolytic loss of H_2O_2 was approximately 3 times that of CH_3OOH. The loss of CH_3OOH through its reaction with HO was about twice the loss of H_2O_2 reacting with HO. This was in agreement with prior O_3-hydroperoxide analyses in the MBL that suggested a stoichiometric conversion of O_3 to hydroperoxides [e.g., *Thompson et al.*, 1993; *Ayers et al.*, 1992].

The rate of surface deposition and the net rate of O_3 photochemical destruction in the MBL, nominally 1.7 × 10^{10} and 5 × 10^{10} molecules cm^{-2} s^{-1}, respectively, can be compared and contrasted with net O_3 production throughout the tropospheric column. *Jacob et al.* [this issue] has presented and discussed tropospheric column net O_3 production throughout the TRACE A study region. They gave an estimated stratospheric source of 1–3 × 10^{10} molecules cm^{-2} s^{-1}, a median net O_3 production rate of 4 × 10^{10} molecules cm^{-2} s^{-1}, and a median gross production rate of 9 × 10^{11} molecules cm^{-2} s^{-1}. The O_3 surface loss rate given above was comparable to the rate of stratospheric injection. MBL O_3 production can be compared with the rest of the tropospheric column and is illustrated for cases *d* and *i* in Figure 7. The vertically integrated net O_3 production for cases *d* (0–8.5 km) and *i* (0–10.5 km) was −6 × 10^{10} and −60 × 10^{10} molecules cm^{-2} s^{-1}. Case *d* was representative of profiles at cases *a*–*f*, *h*, *j*, and *k*. Cases *i* and *g* were similar to each other. Cases *l* and *m* went unanalyzed due to the absence of key species measurements throughout the column. Over the ocean, net O_3 production was negative with the bulk of the O_3 destroyed within or just above the MBL. The highest destruction rates in cases *i* (Figure 7 (right)) and *g* (not shown) were just above a marine stratus cloud deck, were due to the resulting significant enhancement of O_3 photolysis rates, and were associated with some of the highest hydroperoxide concentrations recorded. The median profile presented by *Jacob et al.* [this issue] and representing the

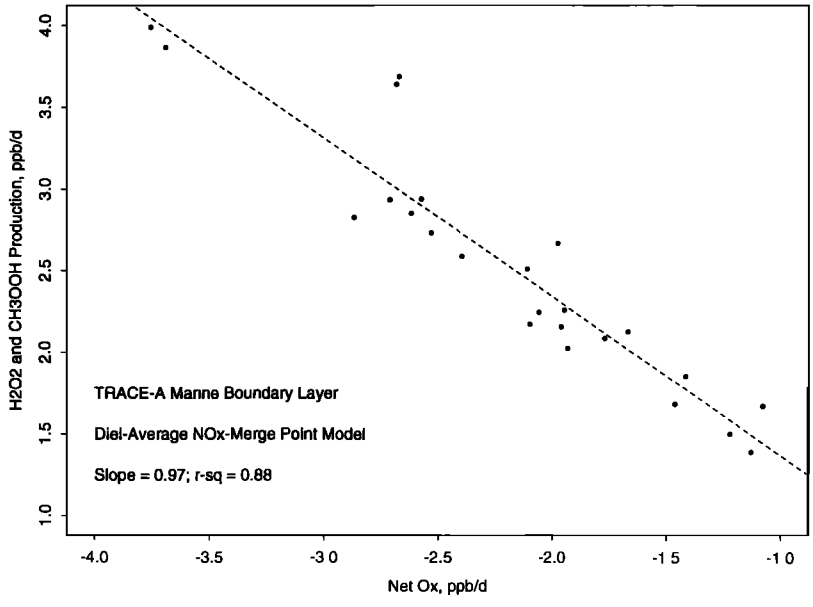

Figure 6. Relationship between H_2O_2 and CH_3OOH gross production and the net O_3 production for all modeled points in the MBL. The solid line shows the least squares linear fit through the data. The slope of the line is −1.0 and the coefficient of determination is 0.83. The photochemical destruction of O_3 is balanced by the net production of the hydroperoxides.

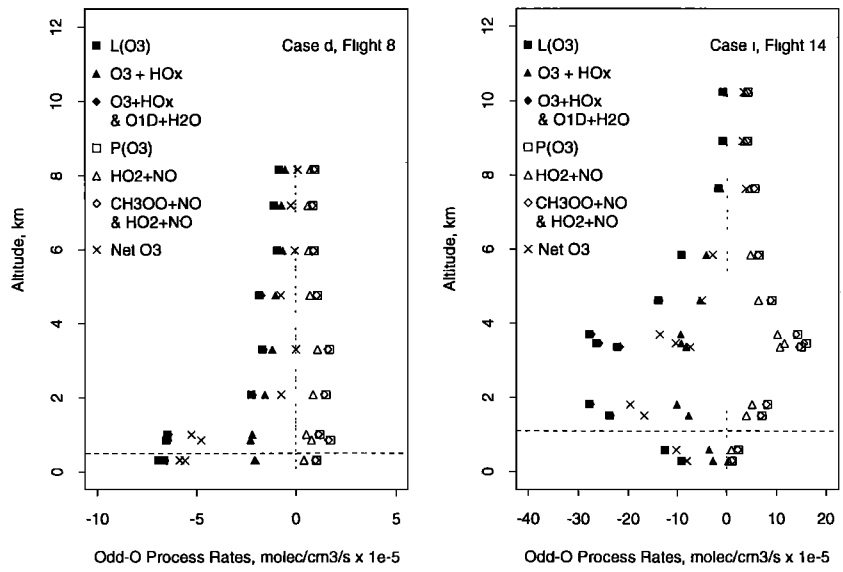

Figure 7. O_3 production as a function of altitude for MBL cases *d* and *i*. Dashed line, net O_3 production; solid square, gross O_3 loss rate; solid triangle, rate of O_3 + HO and O_3 + HO_2; solid diamond, rate of O_3 + HO, O_3 + HO_2 and O^1D + H_2O; open square, gross O_3 formation rate; open triangle, rate of NO + HO_2; open diamond, rate of NO + HO_2 and NO + CH_3OO. Net O_3 destruction occurs principally in the MBL and lower FT and primarily through the reaction of O^1D with water vapor. Note column-integrated destruction of O_3.

TRACE A study region showed a similar trend with altitude but with net column O_3 production near zero. This indicated the South Atlantic basin was near O_3 steady state during the TRACE A period.

The key reactions contributing to net O_3 production are detailed in Figure 7. CH_3OO and HO_2 radicals contributed equally to gross O_3 production in the MBL. Above the MBL, HO_2 was diagnosed as the primary source of gross O_3 production. O^1D-H_2O and O_3-odd H reactions were the principal O_3 destruction reactions with the former being greater at low altitude. In case *d* the predominance of O^1D-H_2O in the gross destruction of O_3 was limited to altitudes below 2 km and in case *i* its predominance extended up to 7 km, as was discussed above. Gross O_3 production was nearly in balance with O_3-odd H destruction at all altitudes and it is the reaction of O^1D with water which shifted the balance toward net O_3 destruction in these marine profiles.

3.2. NO – NO_2 – PAN – HNO_3

NO is required for O_3 production in the troposphere and its absence or very low concentration, along with H_2O, was responsible for net O_3 loss in the MBL. Even though the TRACE A MBL was depleted in NO and NO_2, there was still considerable movement in the oxides of nitrogen from the lower FT to the MBL and on into the ocean. This is shown schematically in Figure 8. The downward transport of peroxyacetylnitrate (PAN), which comprises most of the oxides of nitrogen flux, exceeded the rate of HNO_3 production and its transport and thermal decomposition was sufficient to maintain observed NO and NO_2 levels without having to invoke an oceanic source for NO. However, the predicted rate of HNO_3 formation from NO_2 and the entrainment of HNO_3 from aloft were significantly lower than the deposition rate of HNO_3 and inadequate to maintain observed levels of HNO_3. Figure 8 also gives lower limits for the air-sea flux of PAN and NO_x. These fluxes were considered of minor importance and were estimated assuming an upper limit deposition velocity of 1 cm s^{-1}.

The deposition of HNO_3 is complicated by the presence of sea-salt aerosol and its absorption of HNO_3 vapor [*Thompson and Zafiriou*, 1983; *Duce et al.*, 1991]. The deposition rate of aerosol varies as a function of particle size and can be consid-

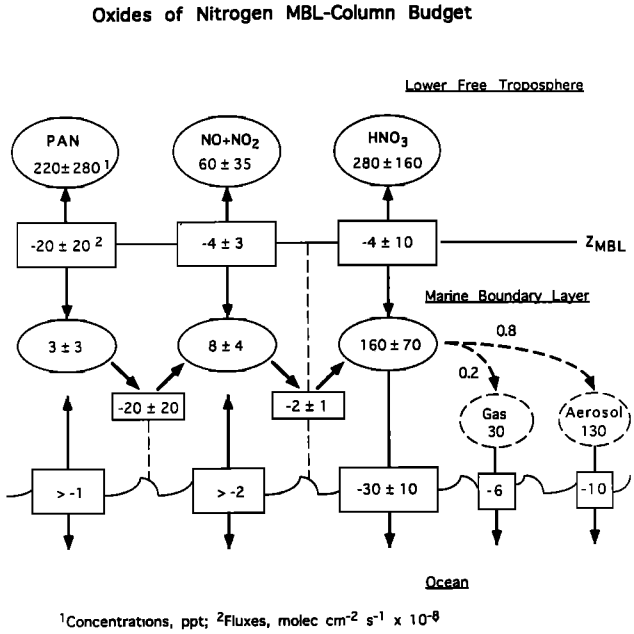

Figure 8. As in Figure 5 except for oxides of nitrogen. Concentrations are in ppt. Dashed arrows and ellipses indicate the unresolved involvement of aerosols in the deposition of HNO_3 and the 0.2 and 0.8 give the assumed partitioning of HNO_3 between gas and aerosol near the surface.

Table 4. Average Column MBL-FT and Oceanic Flux Estimates

Species	C_2H_4	C_3H_6	C_2H_6	C_3H_8	n-C_4H_{10},[a]
Species loss by HO (mean diel-average HO = ~1.5 × 10^6)	280	290	230	80	50
FT-MBL flux (K = 0.5 cm s^{-1})	10	−20	410	50	10
Estimated oceanic source (HO = 1.5 × 10^6) − (FT-MBL flux)	270	310	0	20	0
Plass et al. [1992]	170	85	41	17	3
Donahue and Prinn [1990]	5400	8800	270	560	2500
Bonsang et al. [1988][b]	2300	1100	660	370	170
Lamontagne et al. [1974][b]	600	300	30	45	15
Thompson et al. [1993][c]	360	360	1400	200	
Donahue and Prinn [1993]	180–350	70–160			

In molecules cm^{-2} s^{-1} × 10^{-6}.
[a]Only 5 of 13 MBL cases have data in both MBL and FT.
[b]Calculated by *Donahue and Prinn* [1990] from the data of *Bonsang et al.* [1988] and *Lamontagne et al.* [1974].
[c]GSFC one-dimensional model results for a TRACE A MBL simulation. The model is described by *Thompson et al.* [1993], but the kinetic rate constants and photophysical parameters have been updated per *Atkinson et al.* [1993].

erably different than a gas. Theoretically, the partitioning of HNO_3 between gas and aerosol is a function of particle mass, composition, and relative humidity. A solution to the HNO_3-aerosol deposition problem was presented by *Duce et al.* [1991] and was similar to that used by *Thompson and Zafiriou* [1983]. Duce et al. assumed, based on shipboard and island observations, 15% of the total nitrate (HNO_3 plus aerosol nitrate) in the MBL to be in the gas phase and the remainder to be distributed on the sea-salt aerosol. A mean aerosol deposition velocity of 0.3 cm s^{-1} was also assumed. *Papenbrock et al.* [1992] presented data from a cruise in the South Atlantic during September and October 1988, which showed 10–20% of the total nitrate to be in the gas phase, consistent with the Duce et al. assumption. Their cruise track is shown by the dashed line on Figure 1. The Papenbrock et al. gas and aerosol concentrations (measured at a height 20 m above the ocean), ranged from <30–70 ppt to 40–700 ppt, respectively, and the HNO_3 at 300 m in TRACE A was within the range of their total nitrate concentration. After assuming 20% of the HNO_3 measured at 300 m remains as a gas, the remainder absorbs onto aerosols, and the aerosol deposition rate is 0.3 cm s^{-1}, then the resultant HNO_3 and aerosol nitrate fluxes are 6×10^8 and 10×10^8 molecules cm^{-2} s^{-1}. The effect of aerosol is indicated in Figure 8 by the dashed boxes, ellipses, and arrows. These fluxes represent lower limits only, since we did not measure and have not included aerosol nitrate at 300 m in the MBL flux estimates. The inclusion of aerosol effects puts in balance the MBL NO_x-HNO_3-PAN system and the oxide of nitrogen family appears to be near steady state. In TRACE A the deposition of nitrate appears to be limited by the entrainment of the oxides of nitrogen and not by surface deposition nor by photochemical oxidation of NO_2.

The estimated dry deposition flux of HNO_3 gas to the South Atlantic during TRACE A, $3 \pm 2 \times 10^9$ molecules cm^{-2} s^{-1}, was about 10 times the annual average estimate for this region. The aerosol and gas deposition estimate was comparable to the deposition rate for all nitrate-containing species, 2×10^9 molecules cm^{-2} s^{-1} [*Duce et al.*, 1991].

3.3. Light Hydrocarbons, $<C_4$

The surface emission rates of hydrocarbons were estimated from their MBL concentration, reactivity with O_3 and HO, and rate of entrainment from aloft, as was done by *Donahue and Prinn* [1990]. In this scheme the MBL hydrocarbon species are assumed to be in steady state such that the ocean or FT supplies them at a rate equal to their photochemical destruction. The concentration of O_3 was taken from the observations and the photochemical model was used to estimate HO and NO_3 in the MBL. Hydrocarbon oxidation by NO_3 could be neglected in the TRACE A MBL. Kinetic rate constants were taken from *Atkinson et al.* [1993] and evaluated assuming a temperature of 20°C and a pressure of 950 hPa. The average MBL column chemical destruction rates for C_2H_4, C_2H_6, C_2H_6, C_3H_8, and n-C_4H_{10} during TRACE A are listed in Table 4. The diel-average HO concentration was ~1.5×10^6 and the midday HO concentration was ~5×10^6. The oceanic sources implied by the chemical destruction rates should be reduced by an amount equal to the FT-MBL entrainment rates, which are listed in Table 4, and the differences yield refined estimates of the oceanic emission rates. For C_2H_4 and C_3H_6 the inferred oceanic source was an order of magnitude larger than the estimated FT source, clearly demonstrating the ocean as the source of these compounds. There was a progression in the alkanes from those indicating a predominantly oceanic source, n-C_4H_{10}, to those with an equal likelihood of an oceanic or FT source, C_3H_8, and on to those suggesting a predominantly FT source, C_2H_6. *Plass et al.* [1992] estimated the oceanic flux of these hydrocarbons for the South Atlantic from surface seawater and lower MBL measurements (cruise track is shown in Figure 1). Their data are also listed in Table 4. The TRACE A lower-limit rate for C_2H_4 was comparable to theirs, but our estimated oceanic fluxes for the other species were 2–4 times their flux estimates. *Donahue and Prinn* [1990] determined hydrocarbon fluxes for the remote MBL from their own model analysis and from the measurements of *Bonsang et al.* [1988] and *Lamontagne et al.* [1974]. Their C_2H_4 and C_3H_6 flux estimates were significantly greater (~10 times) than those given here and their alkane fluxes were similar in magnitude but higher (approximately a factor of 2–4). The high rates reflected the inclusion in their "base case" of the significantly higher atmospheric hydrocarbon concentrations reported by Bonsang et al. as compared to others [*Singh and Zimmerman*, 1992]. *Donahue and Prinn* [1993] calculated ocean fluxes of

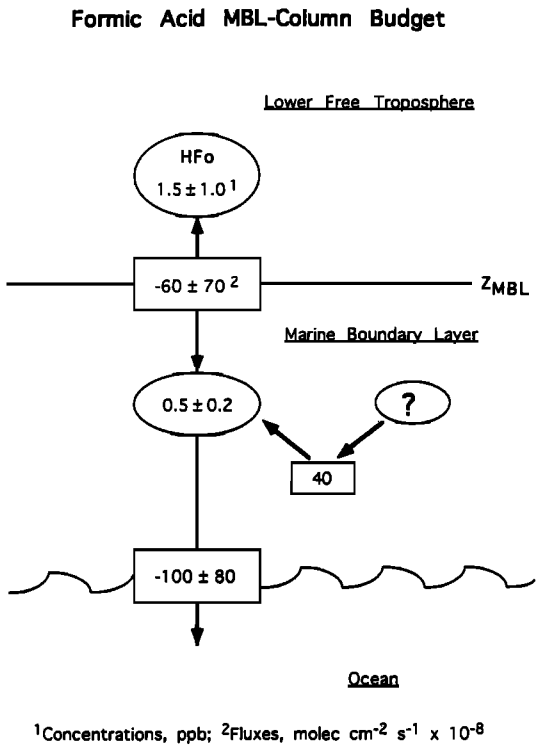

Figure 9. As in Figure 5 except for formic acid.

C_2H_4 and C_3H_6 for the equatorial Pacific based upon their own seawater and atmospheric concentrations and measured winds. Their flux estimates were comparable to those reported here and by Plass et al. *Thompson et al.* [1993] also calculated hydrocarbon flux estimates for SAGA 3 using the Goddard Space Flight Center (GSFC) one-dimensional photochemical model. Their flux estimates are higher than those of *Donahue and Prinn* [1993]. This result was due, in part, to matching different hydrocarbon data sets [*Donahue and Prinn*, 1993; *Atlas et al.*, 1993], differences in model mechanisms and differences in model HO. The GSFC one-dimensional model was applied to the TRACE A MBL data and yielded alkene fluxes, which were of the same order as the point model but gave much higher fluxes for the alkanes. These flux estimates are listed in Table 4.

3.4. CH_2O and Formic Acid – HFo

In TRACE A, HFo was significantly greater in the lower FT than in the MBL due to the transport of continental emissions [*Talbot et al.*, this issue]. Figure 9 shows the HFo MBL budget. The FT-MBL flux of HFo is approximately 1/2 of the MBL deposition flux of HFo. This suggests an in situ source of HFo of the order of 6×10^4 molecules cm^{-3} s^{-1} or ~200 ppt d^{-1}.

Tokos [1989] proposed HFo to have a photochemical source, based upon his observations of its diel cycle in the MBL over the Atlantic in the summer of 1988. He suggested a likely mechanism was heterogeneous photochemical conversion of CH_2O to HFo in cloud or aerosol, as was modeled by *Chameides and Davis* [1983] and *Jacob* [1986]. *Arlander et al.* [1990] also noted a diel cycle in HFo and postulated that it arose from either vertical transport phenomena or sunlight-driven activity (photochemistry and biological activity). Heterogeneous photochemistry was stated by them to be unable to yield sufficient HFo. *Talbot et al.* [1990, 1995a] and *Keene et al.* [1995] have also shown that aqueous chemistry cannot explain observations of HFo in the Amazonian dry and wet seasons nor in the fall at Shenandoah National Park. *Arlander et al.* [1990] concluded that a more likely MBL source was the gas phase ozonolysis of alkenes, C_2H_4 or C_3H_6, since a correlation among alkenes, HFo, HAc, and CH_2O was observed. In TRACE A, however, the above diagnosed oceanic emission rates for these compounds and those from *Plass et al.* [1992] would be insufficient to support HFo production via their oxidation. The upper limit total oceanic emissions of alkenes (17×10^8 molecules cm^{-2} s^{-1}, Table 4) were less than 1/2 of that required, 40×10^8 (Figure 9). A viable gas phase or aqueous photochemical source of HFo remains to be demonstrated.

The available CH_2O measurements within the MBL and lower FT are listed in Table 3. The CH_2O instrument duty cycle, 10 min of measurements followed by 10 min of background, and the short residence time of the aircraft in the MBL, often <5 min, combined to reduce the number of MBL cases with CH_2O data. It was unreasonable to perform CH_2O budget calculations on so few cases.

The low CH_2O concentrations were striking and significantly below (factors of 2–10) those predicted by the photochemical model. *Jacob et al.* [this issue] have discussed this discrepancy in terms of gas phase mechanisms and measurement uncertainty. The inclusion of a surface loss process in the point model brought its predicted concentrations down slightly, a few tens of percent, but nowhere near the factors of 2 to 3 required. The CH_2O concentrations of cases *a* and *e*, 230 and 170 ppt, respectively, were comparable to (1) the cleaner air data of *Lowe and Schmidt* [1983] from a cruise near the Brazilian coast in October and November 1980, (2) the South Atlantic clean air data reported by *Carlier et al.* [1990] from a cruise in October 1988, and (3) the very clean air measurements of *Arlander et al.* [1990] over the Indian Ocean near western Australia. However, the values below the detection limit, nominally 45 ppt, for cases *h*, *i*, *j*, *l*, and *m* were well below these measurements. The latter measurements imply either measurement uncertainty was greater than realized or a process related to CH_2O formation or loss is absent from the model.

4. Discussion

The simple FT-MBL and surface flux models and the photochemical point model provided a framework from which to discuss the chemical budgets of ozone, hydroperoxides, oxides of nitrogen, and hydrocarbons. The MBL budgets of O_3 and hydroperoxides appeared to be in reasonable balance. The close correspondence between measured and model values of H_2O_2, CH_3OOH, and CH_2O above the MBL indicated that the photochemical model chemical mechanisms and kinetic rate constants captured the odd hydrogen and odd oxygen chemistry of the FT [*Jacob et al.*, this issue]. The O_3, H_2O_2, and CH_3OOH MBL measurements and model results, including MBL flux estimates, suggested that this result applied in the MBL as well. The estimated surface deposition velocity together with a mean MBL height yield pseudo-first-order loss rates of 1.4×10^{-5} s^{-1} for HFo, HNO_3, CH_2O, and H_2O_2, and 6×10^{-6} s^{-1} for CH_3OOH. The surface loss rate of H_2O_2 was approximately twice its diel-average photochemical loss rate. For CH_3OOH, surface deposition was about 1/2 its diel-average photochemical loss rate and that for CH_2O was about 1/3 its diel-average photochemical loss rate. The inclusion of

surface deposition in the point model reduced the instantaneous steady state values of H_2O_2, CH_3OOH, and CH_2O to 1/2, 2/3, and 3/4 of their values without surface deposition. Modeled and measured concentrations of H_2O_2 and CH_3OOH were resolved with surface deposition, whereas model CH_2O remains significantly greater than the measured values. In total, the oxides of nitrogen family was balanced in the MBL, but this required the inclusion of gas-aerosol partitioning for HNO_3 and an additional mechanism for converting PAN to HNO_3 is needed.

The lack of model-measurement closure in CH_2O was consistent with observations at Mauna Loa Observatory and model simulations of the chemistry of this location [*Heikes*, 1992; *Liu et al.*, 1992; *Heikes et al.*, 1996]. The CH_2O analytical method used during TRACE A was also used in a series of CH_2O methods comparisons at Mauna Loa Observatory [*Heikes et al.*, 1996]. It consistently gave results which were the same (within estimated instrumental precision) or higher in value than the other measurements. Hence it was considered to provide an upper limit to ambient CH_2O there.

A HFo formation mechanism operative in the MBL has yet to be identified. The magnitudes of the missing CH_2O sink and HFo source were comparable. While intriguing, whether the missing CH_2O sink and HFo source are related and whether this relationship was a consequence of the low NO environment may have been fortuitous and cannot be firmly established here. However, the role of heterogeneous chemistry on CH_2O and HFo in a cloud-impacted MBL is the subject of future work.

5. Conclusions

Chemical budgets were constructed for several species in the MBL and presented for ethane, ethylene, propane, propylene, *n*-butane, formic acid (HFo), methylhydroperoxide, oxides of nitrogen (i.e., NO, NO_2, PAN, HNO_3), hydrogen peroxide, and ozone. A diel-average photochemical point model was used to evaluate local photochemical production and loss of these species. An entrainment model was used to estimate material exchange between the lower free troposphere and MBL and a resistance deposition model was used to calculate material exchange across the air-sea interface. The results suggested the ocean to be the source of measured alkenes in the MBL and that the ocean is the most likely source of the shorter-lived alkanes: propane and *n*-butane with a smaller contribution from the FT. The estimated hydrocarbon sources from the ocean were in agreement with prior analyses. Transport from the lower FT together with surface loss could not account for measured concentrations of HFo and HNO_3. A photochemical source of HFo is needed in the MBL. The transport of PAN from the FT to the MBL exceeds the rate of NO_2 oxidation to HNO_3 and was more than sufficient to maintain observed NO_x levels without having to invoke an oceanic source for NO. The total flux of the sum of NO_x, PAN, and HNO_3 was in balance with the surface deposition flux of HNO_3 and indicated balance of the oxides of nitrogen family. However, the predicted rates of HNO_3 formation and HNO_3 entrainment from aloft were inadequate to maintain observed levels of HNO_3 unless aerosol partitioning and depositional effects were included. The estimated dry deposition flux of HNO_3 to the South Atlantic during TRACE A was about 10 times the annual average estimate for this region and comparable to the deposition rate for all nitrate-containing species. The destruction of O_3 within the MBL was more than balanced by transport from aloft. The principal destruction process was through photochemical reactions and mediated by the formation and surface deposition of H_2O_2 and CH_3OOH. A direct loss of ozone to the sea surface was of secondary importance. CH_3OOH loss to the sea surface and its transport into the FT from the MBL was estimated to occur at a first-order loss rate of 6×10^{-6} s^{-1} for a mean MBL height of 700 m. H_2O_2, HFo, HNO_3 and CH_2O losses from the MBL are estimated at rates of 1.4×10^{-5} s^{-1}. Sea-salt aerosol confounds the surface deposition of HNO_3. Inclusion of surface loss improved the agreement between model-predicted and measured concentrations of HNO_3, CH_3OOH, H_2O_2, and CH_2O, species which had been overestimated in the MBL by the photochemical point model. A strong but unknown CH_2O sink was required in addition to surface deposition to resolve model and measurements in the MBL. The missing sink of CH_2O and source of HFo were comparable.

References

Arlander, D. W., D. R. Cronin, J. C. Farmer, F. A. Menzia, and H. H. Westberg, Gaseous oxygenated hydrocarbons in the remote troposphere, *J. Geophys. Res.*, *95*, 16,391–16,403, 1990.

Atkinson, R., D. L. Baulch, R. A. Cox, R. F. Hampson Jr., J. A. Kerr, and J. Troe, Evaluated kinetic and photochemical data for atmospheric chemistry, supplement IV, IUPAC subcommittee on gas kinetic data evaluation for atmospheric chemistry, *J. Phys. Chem. Ref. Data*, *21*, 1125–1568, 1993.

Atlas, E., W. Pollock, J. Greenberg, L. Heidt, and A. M. Thompson, Alkyl nitrates, nonmethane hydrocarbons, and halocarbon gases over the equatorial Pacific Ocean during SAGA 3, *J. Geophys. Res.*, *98*, 16,933–16,948, 1993.

Ayers, G. P., S. A. Penkett, R. W. Gillett, B. Bandy, I. E. Galbally, C. P. Meyer, C. M. Ellsworth, S. T. Bentley, and B. W. Forgan, Evidence for photochemical control of ozone concentrations in unpolluted marine air, *Nature*, *360*, 446–448, 1992.

Ayers, G. P., S. A. Penkett, R. W. Gillett, and B. Bandy, Cape Grimm ozone-hydrogen peroxide data, *J. Geophys. Res.*, in press, 1995.

Blake, N. J., D. R. Blake, B. C. Sive, T.-Y. Chen, F. S. Rowland, J. E. Collins, G. W. Sachse, and B. E. Anderson, Biomass burning emissions and vertical distribution of atmospheric methy halides and other reduced carbon gases in the South Atlantic region, *J. Geophys. Res.*, this issue.

Bonsang, B., M. Kanakidou, G. Lambert, and P. Monfray, The marine source of C_2-C_6 aliphatic hydrocarbons, *J. Atmos. Chem.*, *6*, 3–20, 1988.

Bonsang, B., et al., Vertical distribution of nonmethane hydrocarbons in the remote marine boundary layer, *J. Geophys. Res.*, *96*, 7313–7324, 1991.

Bretherton, C. S., and S. T. Siems, Cloudiness and marine boundary layer dynamics in the ASTEX Lagrangian experiments, in *Proceedings of the Sixth Conference on Climate Variations*, pp. 323–326, Am. Meteorol. Soc., Boston, Mass., 1994.

Bretherton, C. S., P. Austin, and S. T. Siems, Cloudiness and marine boundary layer dynamics in the ASTEX Lagrangian experiments, II, Cloudiness, drizzle, surface fluxes, and entrainment, *J. Atmos. Sci.*, in press, 1995.

Browell, E. V., et al., Ozone and aerosol distributions and air mass characteristics observed over the South Atlantic basin, during the burning season, *J. Geophys. Res.*, this issue.

Carlier, P., P. Fresnet, V. Lescoat, S. Pashalidis, and G. Mouvier, Formaldehyde background levels over the Atlantic Ocean during the *Polarstern* crossing from Bremerhaven to Rio Grand Do Sol, in *Physico-Chemico Behavior of Atmospheric Pollutants*, pp. 669–674, Kluwer Acad., Norwell, Mass., 1990.

Chameides, W. L., and D. D. Davis, Aqueous phase source of formic acid in clouds, *Nature*, *304*, 427–429, 1983.

Collins, J., et al., CO, O_3, dew point correlations during ABLE 2B and TRACE A, *J. Geophys. Res.*, this issue.

Crawford, J., et al., A photostationary state analysis of the NO-NO_2 system based on airborne observations from the western and central North Pacific, *J. Geophys. Res.*, *101*, 2053–2072, 1996.

Donahue, N. M., and R. G. Prinn, Nonmethane hydrocarbon chemistry in the remote marine boundary layer, *J. Geophys. Res.*, *95*, 18,387–18,411, 1990.

Donahue, N. M., and R. G. Prinn, In situ nonmethane hydrocarbon measurements on SAGA 3, *J. Geophys. Res.*, *98*, 16,915–16,932, 1993.

Duce, R. A., et al., The atmospheric input of trace species to the world ocean, *Global Biogeochem. Cycles*, *5*, 191–259, 1991.

Fishman, J., C. E. Watson, J. C. Larsen, and J. A. Logan, Distribution of tropospheric ozone determined from satellite data, *J. Geophys. Res.*, *95*, 3599–3617, 1990.

Fishman, J., et al., NASA GTE TRACE A experiment (September–October 1992): Overview, *J. Geophys. Res.*, this issue(a).

Fishman, J. V. G. Brackett, E. V. Browell, and W. B. Grant, Tropospheric ozone derived from TOMS/SBUV measurements during TRACE A, *J. Geophys. Res.*, this issue(b).

Fuelberg, H. E., J. D. VanAusdall, E. V. Browell, and S. P. Longmore, Meteorological conditions associated with vertical distributions of aerosols off the west coast of Africa, *J. Geophys. Res.*, this issue(a).

Fuelberg, H. E., R. O. Loring, M. V. Watson, M. C. Sinha, K. E. Pickering, A. M. Thompson, D. P. McNamara, G. W. Sachse, D. R. Blake, and M. R. Schoeberl, TRACE A trajectory intercomparison, 2, Isentropic and kinematic methods, *J. Geophys. Res.*, this issue(b).

Heikes, B. G., Formaldehyde and hydroperoxides at Mauna Loa Observatory, *J. Geophys. Res.*, *97*, 18,001–18,013, 1992.

Heikes, B. G., et al., Hydrogen peroxide and methylhydroperoxide distributions related to ozone and odd hydrogen over the North Pacific in the fall of 1991, *J. Geophys. Res.*, *101*, 1891–1905, 1996.

Jacob, D. J., Chemistry of HO in remote clouds and its role in the production of formic acid and peroxymonosulfate, *J. Geophys. Res.*, *91*, 9807–9826, 1986.

Jacob, D. J., et al., Origin of ozone and NO_x in the tropical troposphere: A photochemical analysis of aircraft observations over the South Atlantic basin, *J. Geophys. Res.*, this issue.

Kawa, S. R., and R. Pearson Jr., Ozone budgets from the dynamics and chemistry of marine stratocumulus experiment, *J. Geophys. Res.*, *94*, 9809–9817, 1989.

Keene, W. C., et al., Carboxylic acids in clouds at a high-elevation forested site in central Virginia: Phase partioning, thermodynamic relationships, and implications for aqueous phase production, *J. Geophys. Res.*, in press, 1995.

Krishnamurti, T. N., M. C. Sinha, M. Kanamitsu, D. Oosterhof, H. Fuelberg, R. Chatfield, D. J. Jacob, and J. Logan, Passive tracer transports relevant to the TRACE A experiment, *J. Geophys. Res.*, this issue.

Lamontagne, R. A., J. W. Swinnerton, and V. J. Linnebom, C_1-C_4 hydrocarbons in the North and South Pacific, *Tellus*, *26*, 71–77, 1974.

Lazrus, A. L., K. L. Fong, and J. A. Lind, Automated fluorometric determination of formaldehyde in air, *Anal. Chem.*, *60*, 1074–1078, 1988.

Lee, M., B. C. Noone, D. O'Sullivan, and B. G. Heikes, Method for the collection and HPLC analysis of hydrogen peroxide and C_1 and C_2 hydroperoxides in the atmosphere, *J. Atmos. Ocean. Technol.*, *12*, 1060–1070, 1995.

Lenschow, D. H., R. Pearson Jr., and B. B. Stankov, Measurements of ozone vertical flux to ocean and forest, *J. Geophys. Res.*, *87*, 8833–8837, 1983.

Liu, S. C., M. McFarland, D. Kley, O. Zafiriou, and B. Huebert, Tropospheric NO_x and O_3 budgets in the equatorial Pacific, *J. Geophys. Res.*, *85*, 7546–7552, 1983.

Liu, S. C., et al., A study of the photochemistry and ozone budget during the Mauna Loa Observatory Photochemistry Experiment, *J. Geophys. Res.*, *97*, 10,463–10,471, 1992.

Lowe, D., and U. Schmidt, Formaldehyde (HCHO) measurements in the nonurban troposphere, *J. Geophys. Res.*, *88*, 10,844–10,858, 1983.

Mauzerall, D., et al., Relationships between burning emission and photochemical tracers over the South Atlantic, *J. Geophys. Res.*, in press, 1996.

McFarland, M., D. Kley, J. W. Drummond, A. L. Schemltekopf, and R. H. Winkler, Nitric oxide measurements in the equatorial Pacific region, *Geophys. Res. Lett.*, *6*, 605–608, 1979.

Noone, K. J., R. D. Schillawski, G. L. Kok, C. S. Bretherton, and B. J. Huebert, Ozone in the marine atmosphere observed during ASTEX/MAGE, *J. Geophys. Res.*, *101*, 4485–4499, 1996.

O'Sullivan, D., M. Lee, K. B. Noone, and B. G. Heikes, Henry's law solubility of hydrogen peroxide, methylhydroperoxide, hydroxymethyl-hydroperoxide, 1-hydroxyethyl-hydroperoxide, peroxyacetic acid, and ethyl-hydroperoxide, *J. Phys. Chem.*, in press, 1995.

Paluch, I. R., D. H. Lenschow, S. Siems, S. McKeen, G. L. Kok, and R. D. Schillawski, Evolution of the subtropical marine boundary layer: Comparison of soundings over the eastern Pacific from FIRE and HaRP, *J. Atmos. Sci.*, *51*, 1465–1479, 1994.

Papenbrock, T. H., F. Stuhl, K. P. Müller, and J. Rudolph, Measurements of gaseous HNO_3 over the Atlantic Ocean, *J. Atmos. Chem.*, *15*, 369–379, 1992.

Penc, R. S., and B. A. Albrecht, Parametric representation of heat and moisture fluxes in cloud-topped mixed layers, *Boundary Layer Meteorol.*, *38*, 225–248, 1987.

Pickering, K. E., A. M. Thompson, D. P. McNamara, M. R. Schoeberl, H. E. Fuelberg, R. O. Loring Jr., M. V. Watson, K. Fakhruzzaman, and A. S. Bachmeier, TRACE A trajectory intercomparisons, 1, Effects of different input analyses, *J. Geophys. Res.*, this issue.

Piotrowitz, S. R., D. A. Boran, and C. K. Fischer, Ozone in the boundary layer of the equatorial Pacific Ocean, *J. Geophys. Res.*, *91*, 13,113–13,119, 1986.

Plass, C., R. Koppmann, and J. Rudolph, Light hydrocarbons in the surface water of the mid-Atlantic, *J. Atmos. Chem.*, *15*, 235–251, 1992.

Rudolph, J., and J. Johnen, Measurements of light hydrocarbons over the Atlantic in regions of low biogenic activity, *J. Geophys. Res.*, *95*, 20,583–20,591, 1990.

Singh, H. B., and P. B. Zimmerman, Atmospheric distributions and sources of non-methane hydrocarbons, in *Gaseous Pollutants: Characterizations and Cycling*, edited by J. O. Nriagu, pp. 177–235, John Wiley, New York, 1992.

Smyth, S., et al., Factors influencing the upper free tropospheric distribution of reactive nitrogen over the South Atlantic during the TRACE A experiment, *J. Geophys. Res.*, this issue.

Talbot, R. W., M. O. Andreae, H. Berresheim, D. J. Jacob, and Beecher, Sources and sinks of formic, acetic, and pyruvic acids over central Amazonia, 2, Wet season, *J. Geophys. Res.*, *95*, 16,799–16,812, 1990.

Talbot, R., et al., Carboxylic acids in the rural continental atmosphere of the eastern United States during SCAPE, *J. Geophys. Res.*, *100*, 9335, 1995a.

Talbot, R., et al., Chemical characteristics of continental outflow from Asia to the troposphere over the western Pacific during September–October 1991: Results from PEM-West A, *J. Geophys. Res.*, *101*, 1713, 1996.

Talbot, R., et al., Chemical characteristics of continental outflow over the tropical South Atlantic Ocean from Brazil and Africa, *J. Geophys. Res.*, this issue.

Thompson, A. M., and D. H. Lenschow, Mean profiles of trace reactive species in the unpolluted marine surface layer, *J. Geophys. Res.*, *89*, 4788–4796, 1984.

Thompson, A. M., and O. C. Zafiriou, Air-sea fluxes of transient atmospheric species, *J. Geophys. Res.*, *88*, 6696–6708, 1983.

Thompson, A. M., et al., Ozone observations and a model of marine boundary layer photochemistry during SAGA 3, *J. Geophys. Res.*, *98*, 16,955–16,968, 1993.

Thompson, A. M., T. Zenker, G. E. Bodeker, and D. P. McNamara, Ozone over southern Africa during SAFARI 1992/TRACE A, *J. Geophys. Res.*, this issue.

Tokos, J. J., Formic and acetic acids in the boundary layer over the North Atlantic Ocean, Ph.D. thesis, Univ. of Rhode Island, Narragansett, R. I., 1989.

Torres, A. L., and A. M. Thompson, Nitric oxide in the equatorial Pacific boundary layer: SAGA 3 measurements, *J. Geophys. Res.*, *98*, 16,949–16,954, 1993.

U.S. Navy, U.S. Navy Marine climatic atlas of the world, vol. III, in *Indian Ocean, NAVAIR 50-1C-530*, U.S. Govt. Print. Off., Washington, D. C., 1976.

U.S. Navy, U.S. Navy Marine climatic atlas of the world, vol. IV, in *South Atlantic Ocean, NAVAIR 50-1C-531*, U.S. Govt. Print. Off., Washington, D. C., 1978.

Wang, Q., and B. A. Albrecht, Observations of cloud-top entrainment in marine stratocumulus clouds, *J. Atmos. Sci.*, *51*, 1530–1547, 1994.

Wu, J., Sea surface winds—A critical input to oceanic models, but are they accurately measured, *Bull. Am. Meteorol. Soc.*, *76*, 13–19, 1995.

Zafiriou, O. C., and M. McFarland, Nitric oxide from nitrite photolysis in the central equatorial Pacific, *J. Geophys. Res.*, *86*, 3173–3182, 1981.

B. Anderson, NASA Langley Research Center, Hampton, VA 23681-0001.
D. Blake, University of California, Irvine, CA 92717.
J. Bradshaw, Georgia Institute of Technology, Atlanta, GA 30332.
H. Fuelberg, Florida State University, Tallahassee, FL 32306.
B. Heikes (corresponding author), and M. Lee, Center for Atmospheric Chemistry Studies, Graduate School of Oceanography, University of Rhode Island, Narragansett, RI 02882-1197. (email: zagar@notos.gso.uri.edu)
D. Jacob, Harvard University, Cambridge, MA 02138.
H. Singh, NASA Ames Research Center, Moffet Field, CA 94035.
R. Talbot, University of New Hampshire, Durham, NH 03824.
A. M. Thompson, NASA Goddard Space Flight Center, Greenbelt, MD 20771.

(Received March 21, 1995; revised November 6, 1995; accepted November 6, 1995.)